Aerosol Science and Technology

ISSN: 0278-6826 (Print) 1521-7388 (Online) Journal homepage: http://www.tandfonline.com/loi/uast20

Direct measurement of aerosol glass fiber alignment in a DC electric field

Bon Ki Ku, Gregory Deye & Leonid A. Turkevich

To cite this article: Bon Ki Ku, Gregory Deye & Leonid A. Turkevich (2018) Direct measurement of aerosol glass fiber alignment in a DC electric field, Aerosol Science and Technology, 52:2, 123-135, DOI: 10.1080/02786826.2017.1387640

To link to this article: https://doi.org/10.1080/02786826.2017.1387640

AEROSOL SCIENCE AND TECHNOLOGY
2018, VOL. 52, NO. 2, 123–135
https://doi.org/10.1080/02786826.2017.1387640

Direct measurement of aerosol glass fiber alignment in a DC electric field

Bon Ki Ku, Gregory Deye, and Leonid A. Turkevich

Centers for Disease Control and Prevention (CDC), National Institute for Occupational Safety and Health (NIOSH), Division of Applied Research and Technology, Cincinnati, Ohio, USA

ABSTRACT

We report non-conducting aerosol fiber (i.e., glass fiber) alignment in a DC electric field. Direct observation of fiber orientation state is demonstrated and quantitative analysis of fiber alignment is made using phase contrast microscopy in four different conditions: (i) dry air and naturally charged fibers, (ii) humid and naturally charged, (iii) humid and neutralized (Boltzmann charge distribution), and (iv) humid and neutralized with an electrostatic precipitator upstream electrodes (i.e., non-charged). The glass fiber aerosols generated by a vortex shaking method were conditioned using a Po-210 neutralizer or humidifier and were provided into a test unit where cylindrical or parallel plate electrodes are used and high voltage is applied to them. Fibers were collected on a filter immediately downstream from the electrodes and their images were taken through an optical microscope to visualize the fiber orientation and measure the alignment angles and lengths of the fibers. The results showed that under all four conditions tested, airborne glass fibers could be aligned to the electric field with different alignment quality, indicating that the glass fibers can be polarized in a steady electric field. In humid air, the fiber alignment along the field direction was observed to be much better and the number of uniform background particles (i.e., randomly oriented fibers) in angular distributions is smaller than that in dry air. Also, it was found that charged fibers in humid air could be better aligned with negligible uniform background than neutralized and non-charged fibers. Possible mechanisms about humidity and charge effects on enhanced fiber alignment are discussed to support the observations. The results indicate that the enhancement of alignment in an electric field would be possible in humid air for other non-conducting fibrous particles having surface chemistry similar to glass fibers.

ARTICLE HISTORY
Received 10 March 2017
Accepted 20 September 2017

EDITOR
Warren Finlay

1. Introduction

Fiber alignment is a fundamental technology for fiber detection using light scattering in fiber monitoring instruments (Lilienfeld et al. 1979; Lilienfeld 1987) and for fiber length separation by dielectrophoresis (Baron et al. 1994; Deye et al. 1999), and is also important for material synthesis, including composites with a desirable property (Bubke et al. 1997; Martin et al. 2005; Takahashi et al. 2006). Fiber alignment can be made using different external fields such as an electric field (Lilienfeld et al. 1979), magnetic field (Timbrell 1975; Takahashi et al. 2006) and viscous shear flow field (Bernstein and Shapiro 1994). While alignment of fibers depends on their electric, magnetic, or aerodynamic properties in these fields, their alignment in electric and magnetic fields requires two main characteristics of fibers; polarization or magnetization and rotation of fibers, induced and exerted by the external fields. The degree to which an elongated particle (i.e., fiber) can be aligned and rotate to the direction of an applied field depends on effects of the rotating force, i.e., the interaction of the field and the dipole moment induced by polarization (Lilienfeld et al. 1979). Electrical field-induced alignment has been preferentially used for detection of nonspherical particles (Kapustin et al. 1980), and to investigate humidification processes of hygroscopic aerosols (Kapustin and Covert 1980). The theoretical principles underlying the alignment of airborne fibers in electric fields were examined by Fuchs in a study where the degree of particle alignment resulting from the torque exerted by an applied electric field was investigated (Fuchs 1964). Lilienfeld (1985) observed experimentally the straightening of curled asbestos fibers in liquid by electrical field, indicating that axial force exerted by electric field on the fibers makes them aligned to the direction of electric field. Lilienfeld et al. (1979) reported a prototype fibrous aerosol

CONTACT Bon Ki Ku bku@cdc.gov Centers for Disease Control and Prevention (CDC), National Institute for Occupational Safety and Health (NIOSH), 1090 Tusculum Ave, MS-R7, Cincinnati, OH 45226, USA.

Color versions of one or more of the figures in the article can be found online at www.tandfonline.com/uast.

Supplemental data for this article can be accessed on the publisher's website.

monitor capable of selective detection and measurement of airborne fiber-shaped particles using AC electric field applied to quadrupole electrodes. Recently Kim et al. (2007) theoretically studied the alignment of airborne curved carbon nanotube particles undergoing Brownian rotation in a DC electric field. Baron and colleagues (Baron et al. 1994; Deye et al. 1999) developed a fiber length classifier by using dielectrophoresis of fibers in a gradient electric field; the AC electric field polarizes the fibers and aligns them parallel to the field. Although the indirect experimental evidence of the preferential alignment of fibers was reported by researchers, to date, the degree and direction of airborne glass fiber alignment in an electric field have not been quantitatively investigated related to their dependence on charge state and humidity in a systematic way where measurement of the alignment of airborne fibers can be made.

Recently, Ku and colleagues have used screens with different mesh sizes to obtain short fibers by removing longer fibers mostly by interception mechanism (Ku et al. 2014). They demonstrated that using the screen with the blockage on its center could give a relatively sharp cut-off of fiber length because the centrally blocked screen configuration may achieve somewhat greater fiber alignment parallel to the plane of the screen. It is intuitive that the more aligned the fibers are parallel to the screen, the greater their potential for interception by the screen is, which could result in higher selectivity of screens in removing the long fibers. Therefore, in order to improve the efficiency of screens to remove fibers, fiber alignment should be kept parallel to the plane of screens. Thus, for potential application of fiber alignment in an electric field to fiber length classification, it is required to quantitatively examine characteristics of fiber alignment in an electric field.

In this study, we directly demonstrated airborne glass fiber alignment in a DC electric field under four different conditions: (i) dry air and naturally charged fibers, (ii) humid and naturally charged, (iii) humid and neutralized (Boltzmann charge distribution), and (iv) humid and neutralized with an electrostatic precipitator upstream electrodes (i.e., non-charged). Two electrodes pairs, i.e., cylindrical and parallel configurations, were designed to make and quantify the alignment of glass fibers using phase contrast microscopy (PCM). We showed that the degree to which fibers can be aligned and experience rotation to an applied electric field may depend on electrical and surface properties of fibers, e.g., surface charge and surface conductivity due to water layers on the surface.

2. Experimental methods

The test material was glass fiber powder, supplied by the Japan Fibrous Material Research Association (JFMRA) (Kohyama et al. 1997). This same material was used in our recent studies for characterization of airborne fibers (Ku et al. 2013a,b), where glass fiber aerosols were generated by a vortex shaking method. Experimental setup is shown in Figure 1.

Briefly, a weighed amount of the glass fiber powder (i.e., 0.2–0.3 g) was loaded into a vortex shaker tube as received and then was pre-shaked for 30 min by a vortex shaking (Ku et al. 2013b) to fully disperse the powder. The charge condition and humidity of airborne fibers were controlled by a neutralizer (Po-210 strips) and an electrostatic precipitator, and a humidifier consisting of a bubbler and dry air flow, respectively. The relative humidity (RH) of the air flow was measured by a thermohygrometer (Digi-Sense, Cole-Parmer) at room temperature 20°C ± 1. Aerodynamic size distributions of the aerosolized fibers were measured by an aerodynamic particle sizer (APS). In Figure 1, a test unit for fiber alignment is also shown. The test unit is a circular tube with inner diameter of 2.5 cm and length of 5 cm (details for the test unit is described in Figure 2).

Conditioned airborne fibers were provided into the test unit which consists of two electrodes to which high DC voltage is applied by high voltage power supply (negative polarity, 4100 N, EMCO, Sutter Creek, CA, USA). Fibers were collected on a mixed cellulose ester (MCE) filter (25 mm in diameter, pore size: 0.8 μm, Part #: 225–19, SKC Inc., Eighty Four, PA, USA), immediately after the electrodes. It was assumed that the airborne fibers aligned in the field were projected on the filter with their relative direction to the electric field preserved. The aerosol flow rate was 1.5 lpm during the test.

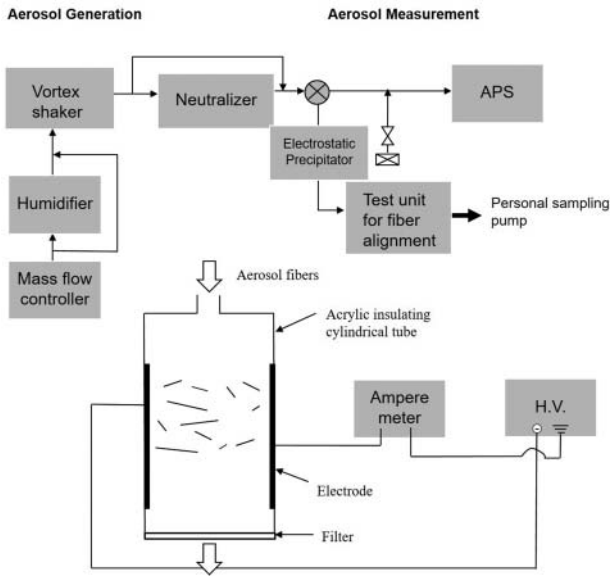

Figure 1. Experimental setup for measurement of fiber alignment (top); Test unit for fiber alignment (bottom).

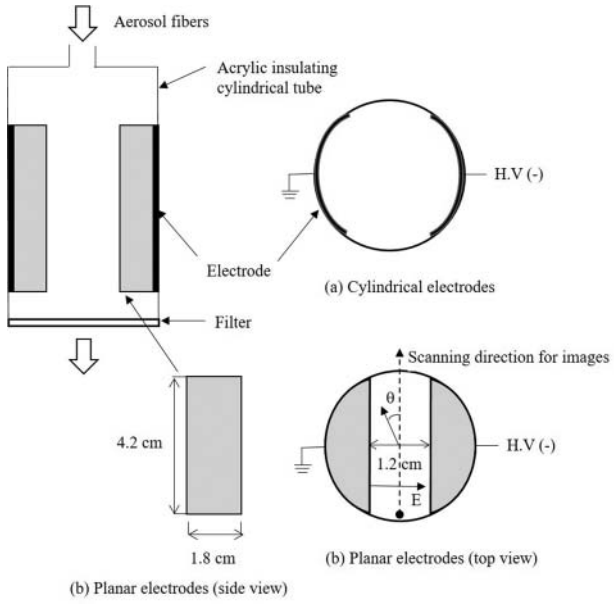

Figure 2. Configuration of a test section for fiber alignment and schematic diagram of cross sections of two types of electrodes. (a) cylindrical electrodes (b) planar electrodes. The arrows mean starting positions and directions which images of fibers on a filter are scanned toward. Alignment angle (θ) of a fiber was measured relatively to the vertical line, as shown in the top view (b). Perfect alignment of a fiber to the electric field (E) is corresponding to 90 degree.

2.1. Two configurations of electrodes

Figure 2 shows two kinds of electrode geometries used to align airborne fibers in the test unit. One is cylindrical and the other is planar. Thin aluminum foil was used to make cylindrical electrodes by covering the inside wall of an insulating acrylic tube whose dimensions are 2.5 cm in diameter and 5 cm long, as shown in Figure 2a. For planar electrodes, two pieces made of acrylic (dimension 1.8 cm × 4.2 cm) were designed, machined and fitted into the insulating tube (Figure 2b). The aluminum foil was attached to the flat surfaces of the pieces to make them conducting. During the test, the current between the two electrodes was monitored by an ampere meter to ensure that there is no electrical discharge at a high voltage applied to the electrodes. The alignment test was performed mostly using the planar electrodes.

2.2. Control parameters

In order to investigate characteristics of fiber alignment in a DC electric filed, we controlled fibers using two parameters: charge state and humidity in the air.

- Charge condition (naturally charged by vortex shaking, neutralized, non-charged)
- Humid condition (dry air (< RH 5%), humid air (RH 90%))

The different conditions for the test are as follows:

i. Dry air and naturally charged fibers (the charge level of the naturally charged fibers was estimated to be in the range from about 7 up to 50 elementary charges. The mean charge level of the naturally charged fibers was estimated by simultaneously measuring the number concentration and total current of the aerosolized fibers using a condensation particle counter (Model 3022, TSI) and aerosol electrometer (Model 3068B, TSI), respectively. From these two measurements, mean charge level per fiber was calculated.)
ii. Humid and naturally charged
iii. Humid and neutralized (i.e., Boltzmann charge distribution)
iv. Humid and neutralized with an electrostatic precipitator upstream electrodes (i.e., non-charged)

In order to examine the charge effect on alignment in this condition, the fibers neutralized through a neutralizer were passed through an electrostatic precipitator (ESP) to select non-charged fibers, and then were sent to the parallel plate electrodes (at 4.5 ∼ 8.4 kV DC between the electrodes with a 1.2 cm gap).

2.3. Visualization of fiber alignment

Visualization and quantification of fiber alignment was done using optical microscope images of the fibers collected on a MCE filter. The fiber-loaded MCE filter needs to be transparent to use phase contrast microscopy for visualization of fiber alignment. Briefly, the filter was exposed to hot acetone vapor. As the acetone vapor permeates the MCE filter, the filter collapses and no longer scatters visible light, and the fibers on the filter can be imaged through an optical microscope. The MCE filter surface has pore structure like a sponge. If the filter were exposed to hot acetone vapor (about 1 mL of liquid acetone is introduced into the top of an ETC Quick Fix acetone vaporizer, Environmental Monitoring Systems, Inc., Charleston, SC), the acetone vapor would permeate the whole surface of the filter and the filter would collapse. The fiber-loaded MCE filter was placed (fiber-side down) on a glass slide, the fibers on the filter lie across the porous surface, and the collapse of the filter will happen in a direction perpendicular to the plane the fibers lie on. Thus, we assume that the collapse of the filter may not affect significantly the fiber orientation if the whole filter surface would collapse at the same rate. The optical images were taken and scanned along the line perpendicular to the electric field line on the filter, as shown in Figure 2b (top view), using a Nikon Labophot-2 microscope, with CCD camera (Moticam 2300, Motic

Instruments, Inc., British Columbia, Canada). This scanning brought out about up to 8 images of the fibers. Most of the images were taken in a bright field with the optical microscope, but some of the images were taken in a dark field to get a good contrast image of the aligned fibers.

2.4. Measurement of fiber alignment angles relative to DC electric field

Fiber alignment angles were measured based on the images taken by the phase contrast microscope using Motic software. About 500–1000 fibers were counted to obtain angular distribution (i.e., alignment probability) statistics: an estimate of the degree of alignment is obtained by fitting the experimental data to a Gaussian (however, there is no theoretical basis for using a Gaussian to describe the alignment effect). It was found that in this range the number of fibers were not significantly fluctuated in each angle bin (10 degrees) due to the small number of fibers counted. Alignment angle (θ) of a fiber was measured relatively to the scanning line of the images, as shown in the top view of Figure 2b. With this defined angle, perfect alignment of a fiber to the electric field is corresponding to 90 degrees. At the same time, the fiber length was measured using the Motic software to investigate the dependence of fiber alignment on its length. Images of fibers with no electric field were used as a control sample.

2.5. Calculation of times for polarization and alignment of fibers in an electric field

The degree to which a needle-shaped particle can be aligned by an electric field depends on the relative influence of fluid shear, thermal energy of the bombarding gas molecules, and electrical energy given to the fiber. The relative importance of two mechanisms such shear alignment and random orientation due to Brownian collisions were assessed using the rotational Peclet number (Pe) proposed by Asgharian and Yu (1989). We calculated the rotational Peclet number, defined as the ratio of velocity gradient (G) to rotational diffusion coefficient (D_r). Assuming a parabolic flow in the test tube (2.2 cm in diameter) and using an air flow rate of 1.5 lpm, the Peclet number is about 1.42 for fibers with aspect ratio of 10, length of 5 μm and diameter of 0.5 μm (see the online supplemental information [SI] for details showing rotational Peclet number as a function of fiber aspect ratio for different fiber diameters). The rotational Peclet number (Pe) increases with both increasing fiber aspect ratio and fiber diameter. For aspect ratio (= 10), Pe is 0.18, 1.42, 11.4 and 90.9, respectively, for fiber diameters (0.25, 0.5, 1.0 and 2.0 μm). For the fibers with smaller diameters (i.e., 0.25 and 0.5 μm), Pe is $\sim$ 1.0 in the aspect ratio range of 10–20. For fiber diameter of 0.25 μm, the Pe is smaller than 1.0 for aspect ratio up to 20. Based on this analysis, Pe number is more dependent on fibers diameter than aspect ratio. According to Asgharian and Yu (1989), flow shear effect on fiber rotation may become important with Pe $\sim$1.0, and when Pe is larger than 1000, the rotation of fiber is completely controlled by the shear flow. However, it is worth noting that for curved aerosol fibers (not ideally straight fibers), they may experience more frequent random orientation in the shear flow (Roschenko et al. 2011) than straight fibers. Considering that Pe number for flow and fibers in our test tube is in the range of 0.1–100, and that the fibers used in the test have a broad distribution of fiber diameters (i.e., 0.1 to 2 μm; geometric mean fiber diameter 0.8 μm) (Kohyama et al. 1997), it is expected that for thin and short fibers, Brownian rotation would be dominant relative to fluid shear while fluid shear alignment becomes dominant with increasing fiber diameter and length.

The relaxation times for polarization and alignment of a fiber can be estimated, assuming electrically conducting fibers (i.e., fibers in humid air), according to Lilienfeld (1985). The polarization time, t_p, required for the free charges on the fiber to move to the opposing ends of the fiber is expressed as follows:

$$t_p = \frac{\varepsilon \rho d}{4} \quad [1]$$

where ε is the dielectric constant of the fiber, ρ is the surface resistivity and d is the fiber diameter.

The relaxation time, t_θ, for alignment of polarized fibers in an electric field for aspect ratio of the fiber $\beta > 10$, is

$$t_\theta = \frac{5.5 \times 10^6}{E^2 \sin 2\theta} \quad [2]$$

where E is the electric field intensity (V/m) and θ is angular measure of orientation with respect to the electric field.

Typical polarization time is of the order of one microsecond for fibers of up to 10 μm in diameter, and alignment time through an angle of one radian would be about 0.5 ms for a field intensity of 1000 V/cm.

The deorientation time, as the fiber leaves the electric field until when it is collected on the filter, is calculated for 20 μm and 10 μm long fibers with fiber diameter of 1 μm using the relation $\overline{\theta^2} = 2kTB_w t$ where $\overline{\theta^2}$ is the mean square angle of rotation of the fiber in a time t and B_w is the rotational mobility (Lilienfeld 1985). This is the time to relax from an aligned orientation to a random orientation by Brownian rotation. The deorientation

time is about 0.18 s and 0.03 s, respectively for 20 μm and 10 μm long fiber of 10 degrees (about 1/6 of a radian). The time from when the fiber leaves the electric field until when it is collected on the filter is about 0.026 s. Based on this, fibers longer than 10 μm may not have a significant effect of deorientation while shorter fibers are expected to experience the deorientation, which may result in some of the broadening in the angular distribution.

Residence time, t_r, of fibers in an electric field in our study is calculated at a given aerosol flow rate of 1.5 lpm.

$$t_r = \frac{V}{Q} \quad [3]$$

where V is volume of electric field space and Q is aerosol flow rate.

The residence time is about 0.36 s. Because the residence time is three orders of magnitude larger than the alignment time and five orders of magnitude larger than the polarization time, we expect alignment of fibers for our experimental geometry.

3. Results

3.1. Visualization of aerosol fiber alignment in an electric field

We investigated the degree of fiber alignment in two electrical field configurations: one is with cylindrical electrodes and the other with parallel electrodes. Figure 3 shows optical images of naturally charged fibers (i.e., as aerosolized by vortex shaking) collected on MCE filter downstream (immediately after) cylindrical electrodes with an applied DC voltage of 8.1 kV (see Figure S1 in the SI for images at 6.4 kV in dry air).

The airborne fibers of almost all lengths except relatively thick fibers are found to be aligned parallel to the applied DC electrical field (see the direction of electric field line shown on the top left of the image). Figures 4 and 5 show the case of parallel plate electrodes in dry air for naturally charged fibers.

Figure 4 shows typical images of the fibers without electric field, which is used as control. Figure 5 shows typical images of the fibers with electric field, and clearly illustrates fiber orientation by a field E = 7.3 kV/cm (fibers are collected on a filter downstream from the electric field), as compared to the random fiber orientation for the case with no electric field (Figure 4). More quantitative analysis of fiber alignment to the electric field is discussed using measured alignment angles in the following section.

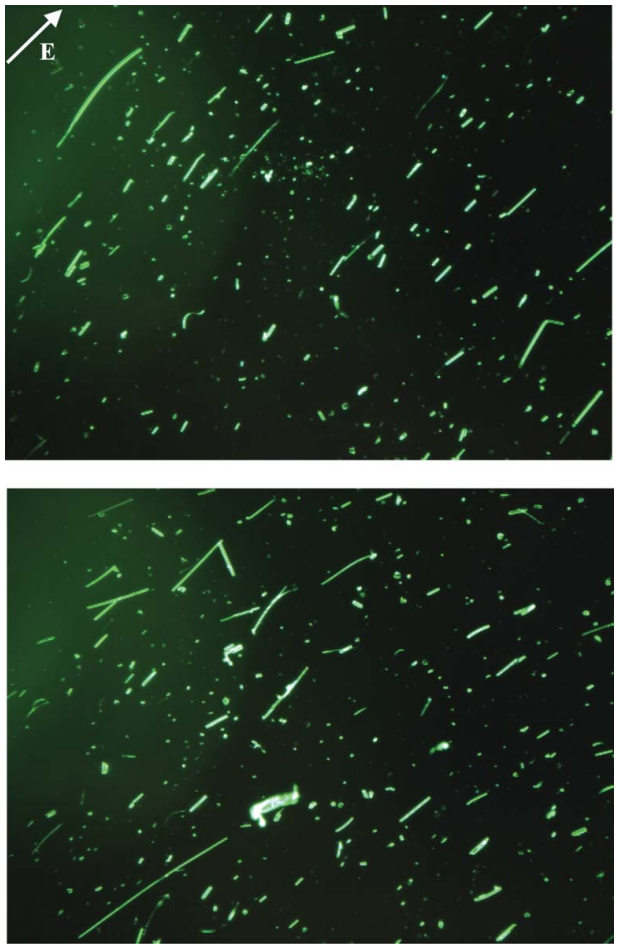

Figure 3. Optical images for fibers collected on MCE filter right after two cylindrical electrodes applied at 8.1 kV of a DC voltage. Naturally charged fibers, dry air and aerosol flow rate 1.5 lpm. Electric field direction is expressed as an arrow on the top left corner of the top image.

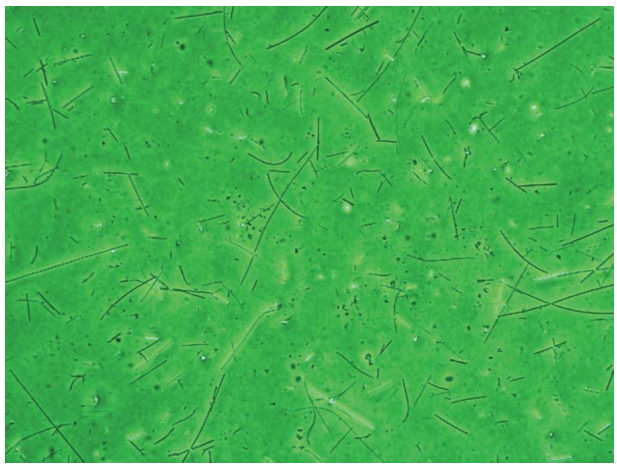

Figure 4. Typical optical image for fibers. Dry air and naturally charged, no electric field in parallel plate electrodes.

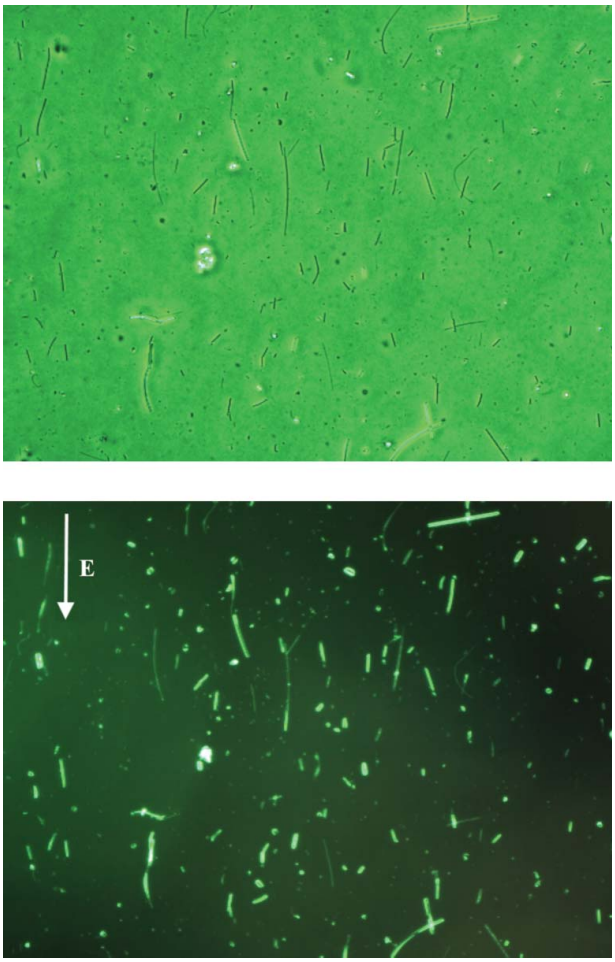

Figure 5. Typical optical images for fibers. Dry air and naturally charged, 7.3 kV on parallel plate electrodes. Bright field image (top) and dark field image (bottom) for the same field of view. Electric field direction is expressed as an arrow on the top left corner of the image.

Figures S2 and S3 in the SI show visualized images of fibers in parallel plate electrodes applied with the same electric field (i.e., 7.3 kV/cm) under humid air condition. For humid and neutralized (Boltzmann charge distribution around zero charge) condition (Figure S2), the images show that the fibers in almost all lengths are aligned to the electric field. For humid and naturally charged fibers (Figure S3), fibers are also aligned well to the field. Compared to the dry condition, the quality of the fiber alignment in humid condition seems to be high. It is worth noting that the aligned fibers in humid condition are relatively short compared to the case of dry condition. This is due to the fact that higher humidity strongly affects particle size distribution and number concentration because the humidity dependence is related to surface chemistry of the material being aerosolized (Ku et al. 2013b). Figure S4 in the SI shows the images of the non-charged fibers collected on a filter, with ESP on upstream parallel plate electrodes. Similar to the conditions of naturally charged or neutralized fibers in humid condition, the non-charged fibers can also be aligned well in humid condition (Figure S4).

3.2. Quantification of aerosol fiber alignment in an electric field for different conditions

To quantify the fiber alignment for different conditions, the angles and lengths of the fibers collected on the MCE filters were measured. Perfect alignment of a fiber to the electric field is corresponding to 90 degrees (Figure 2b). All images scanned along the diameter of the filters were used to obtain representative fiber angle distributions. The finite electrode edge of the parallel plates may distort the electric field because of the finite size effect and thus, the images near at the end of the electrode were excluded.

3.2.1. Alignment of naturally charged fiber in dry condition

Figures 6a and b show angular distributions (number vs. aligned angle) for dry naturally charged fibers without electric field (EF) and with EF, respectively.

Y-axis in Figure 6 is fiber number in each bin (bin size 10 degrees) normalized by total number of fibers counted which was about 1100–2000. The generated fibers with no field would be expected to have a purely random orientation and have a uniform angular distribution. Figure 6a confirms this fact; without electric field, the number-angle distribution as a function of alignment angle is nearly uniform in the range of 0 to 180 degree. This means that fibers become randomly oriented probably due to the relative importance of Brownian motion in the flow compared to the influence of flow velocity gradients and thus the probability for the fibers to have a particular angle in the range is nearly the same. Note that some fibers seem to be slightly aligned in the angle range of 70–100 degrees. This slight alignment might be caused by aerosol encountering the constriction due to the parallel electrodes. When these fibers are exposed to the electric field, the fibers show a preferential alignment to the electric field as shown in Figure 6b. The angular distribution in Figure 6b shows that there is a peak at around 90 degrees and is also some background of randomly oriented fibers. The distribution seems to be symmetric around 90 degrees and the aligned fibers at the peak have three times higher number concentration (i.e., 0.009) than the background (i.e., 0.003). This difference is statistically significant, indicating that fiber alignment do happen in dry and naturally charged condition. The fact that there is background of randomly oriented fibers indicates that not all naturally charged fibers can be aligned in dry air probably because either the electric field is not high enough or the polarization of the non-

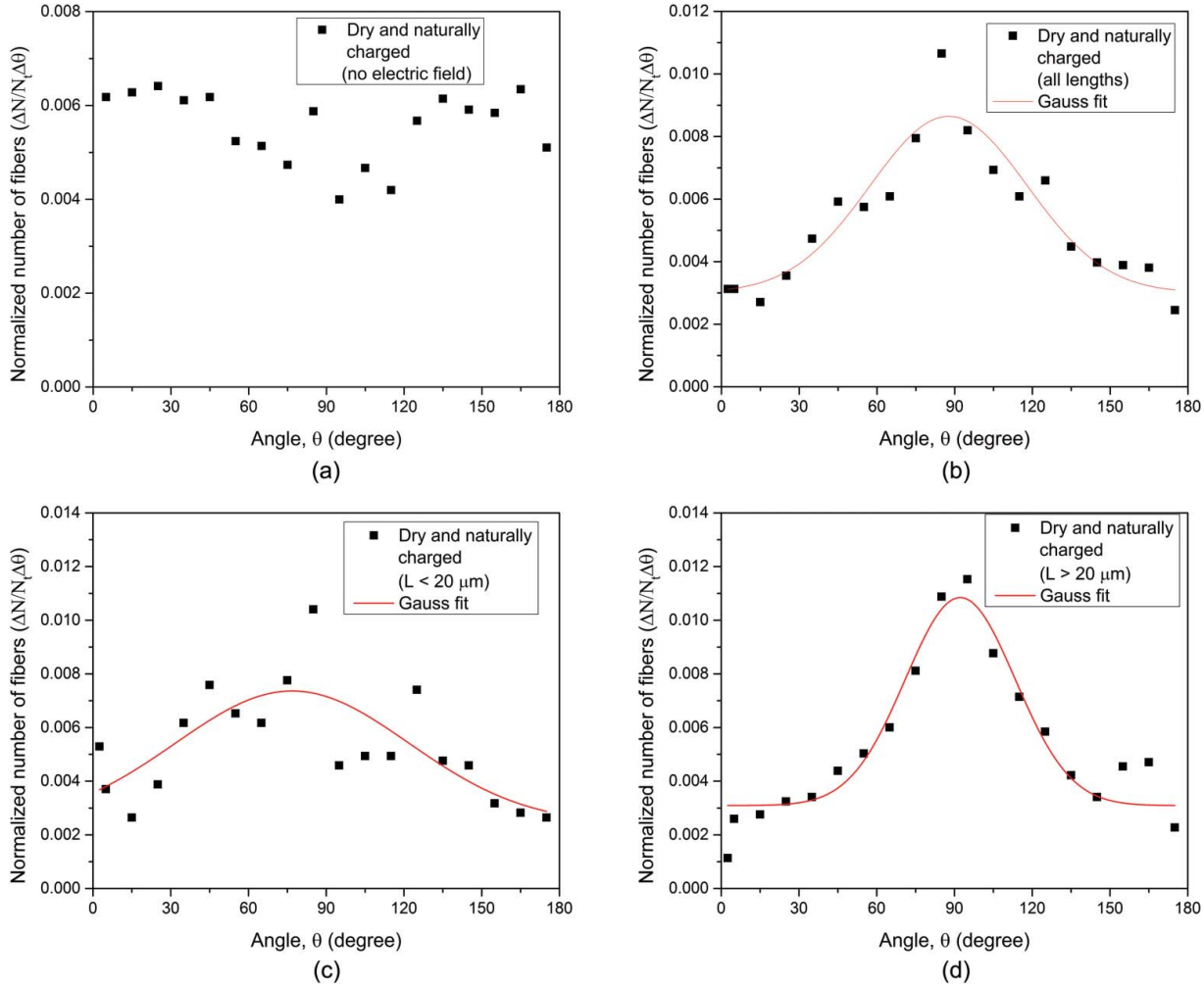

Figure 6. Angular distributions of fibers in dry condition. (a) No electric field, (b) with electric field for all length fibers, (c) with electric field for lengths smaller than 20 μm, and (d) with electric field for lengths larger than 20 μm. N_t is the total number of fibers counted and N is the number of fibers in each angle bin.

conducting glass fibers is not effective to cause them re-orient toward 90 degrees. Nevertheless, Figure 6b clearly shows that the naturally charged fibers can be aligned in a DC electric field even in dry condition.

3.2.2. Dependence of fiber alignment on length

To quantitatively analyze the effect of fiber length on alignment, we split the angle data for dry and naturally charged fibers in the electric field into short (< 20 μm) and long fibers (> 20 μm) and replotted angular distributions for these fiber groups. The length distribution of the aerosolized fibers in dry condition is approximately lognormal, with a geometric mean length (GML) $\sim$ 18.4 μm and geometric standard deviation (GSD) $\sim$ 2.41 (corresponding to the range in the lengths of $\sim$ 1–2 μm up to 100 μm. See Figures 4 and 5 in Ku et al. [2014]). This is in reasonable agreement with the nominal GML $\sim$ 20.0 μm reported for the powder (Kohyama et al. 1997). According to the work of Kohyama et al., the fibers have a geometric mean diameter (GMD) $\sim$ 0.88 μm and GSD $\sim$ 3.1. The rationale for choosing the critical length (20 μm) is based on the fact that a typical macrophage size in the human lung is about 20 μm (Zeidler-Erdely et al. 2006). Fiber length is thought to be an important variable in determining the pathogenicity of asbestos and other elongate mineral particles because the macrophages that normally remove particles from the lungs cannot engulf fibers having lengths greater than the macrophage size. This effect results in greater inflammatory cytokine generation by macrophages exposed to long fibers than to short fibers (Padmore et al. 2017). Macrophages which die in the process of trying to engulf the fibers release additional inflammatory cytokines into the lungs (Blake et al. 1997). Figures 6c and d show angular distributions for short and long fibers, respectively. One distinct thing between the two groups of fibers is that long fibers seem to be aligned a little bit better than short fibers since the aligned peak of the long fibers is

more pronounced relative to the uniform background, and that the uniform background of the short fibers is enhanced relative to the aligned fiber peak. It is suspected that among naturally charged fibers longer fibers may have higher charge than short fibers and thus, more charge on the surface of the longer fiber may increase polarization of the fiber due to non-uniform charge distribution on the surface, which can cause net charge on one end of the fiber. The more net charge on one end of the fiber there is, the stronger the rotating torque on the fiber is.

3.2.3. Effect of relative humidity in air on fiber alignment

We investigated fiber alignment for three different aerosol conditions in humid air; humid and naturally charged fibers, neutralized fibers, and non-charged fibers. Figure 7 shows angular distributions of naturally charged fibers.

Figure 7a clearly shows that naturally charged fibers with all lengths in humid air (RH = 90%) exhibit much stronger alignment than naturally charged fibers in dry air. Alignment along the field direction ($\theta = 90^o$) is more complete (sharper) than for dry fibers, i.e., standard deviation of the angular distribution is 13.7° and 60.7° for humid and dry fibers, respectively (Table 1). Note also the negligible uniform background relative to the number of aligned fibers (i.e., 0.002 vs. 0.043) compared to the dry aerosol (Figure 6b). Figures 7b and c show angular distributions for short ($< 20\ \mu$m) and long fibers ($> 20\ \mu$m), respectively. Contrary to the case of naturally fibers in dry condition, there is little difference between short and long fibers in humid condition; both groups of fibers are equally aligned well to the field with the negligible uniform background. Table 1 summarizes mean aligned angle, standard deviation, and the fraction of background particles for angular distributions fitted with Gaussian distributions for dry and humid conditions.

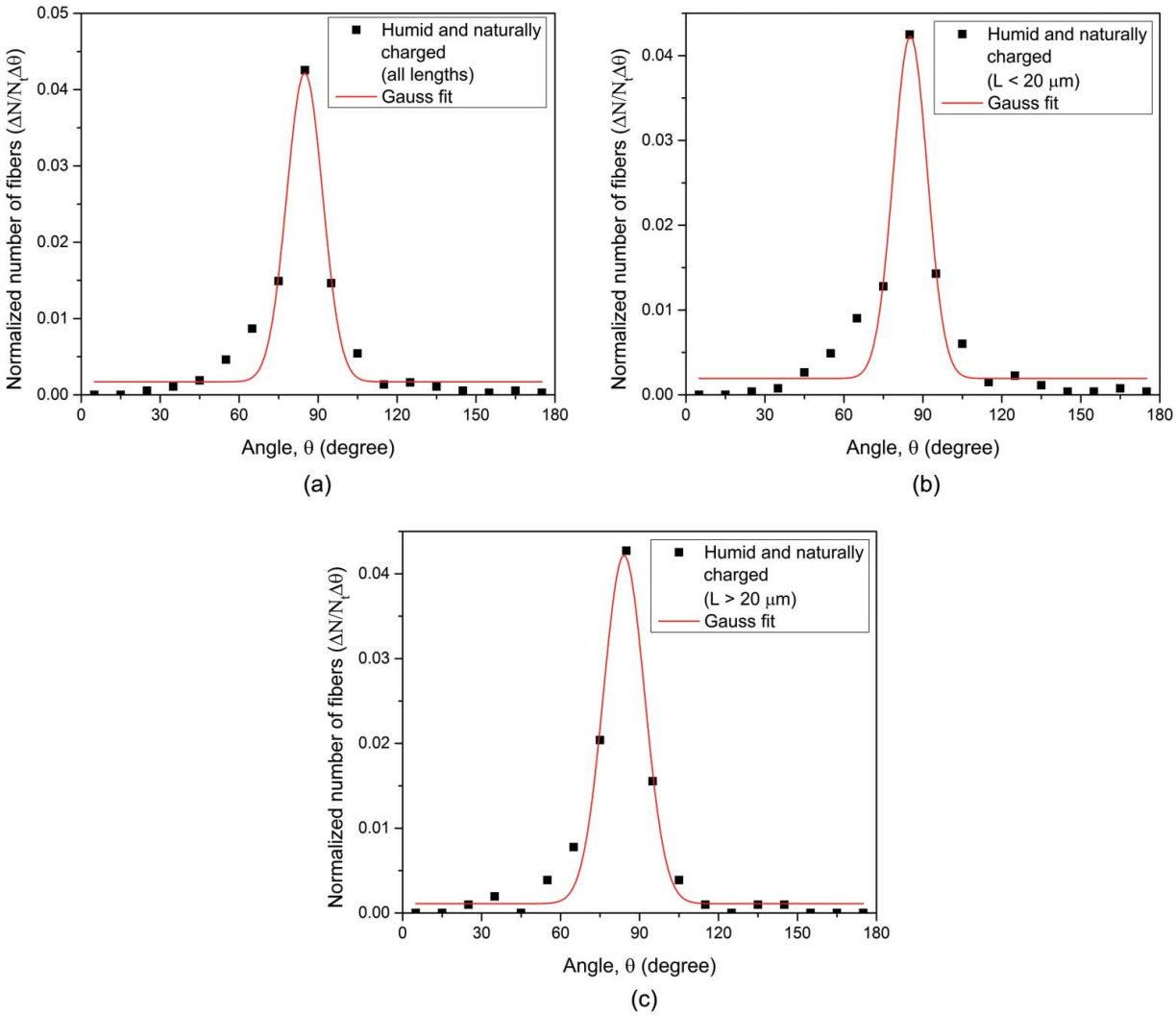

Figure 7. Angular distributions of naturally charged fibers in humid condition. (a) All lengths included, (b) lengths smaller than 20 μm, and (c) lengths larger than 20 μm. N_t is the total number of fibers counted and N is the number of fibers in each angle bin.

Table 1. Mean angle, standard deviation, and background particles for angular distributions fitted with Gaussian distributions for different fiber conditions.

Fiber conditions	Mean angle (degree)	Standard deviation (degree)	Fraction of background particles	Adj. R-Square
Dry and naturally charged (**all length**)	87.6	60.7	0.030	0.8557
Dry and naturally charged (L $<$ 20 μm)	81.3	90.2	0.044	0.4575[a]
Dry and naturally charged (L $>$ 20 μm)	92.2	42.5	0.031	0.9033
Humid and naturally charged (**all length**)	84.9	13.7	0.017	0.9497
Humid and naturally charged (L $<$ 20 μm)	85.2	12.9	0.019	0.9380
Humid and naturally charged (L $>$ 20 μm)	84.1	15.6	0.011	0.9731
Humid and neutralized (Boltzmann) (**all length**)	87.3	39.6	0.017	0.8285
Humid and neutralized (Boltzmann) (L $<$ 20 μm)	84.4	40.2	0.020	0.7028
Humid and neutralized (Boltzmann) (L $>$ 20 μm)	92.1	33.1	0.011	0.9589
Humid and non-charged (**all length**)	79.8	34.7	0.033	0.8490
Humid and non-charged (L $<$ 20 μm)	75.2	38.1	0.040	0.5543[a]
Humid and non-charged (L $>$ 20 μm)	82.1	35.0	0.020	0.9590

[a] The angular distributions were poorly fitted to Gaussian distributions due to the higher uniform background.

The angular distributions of naturally charged fibers in dry and humid conditions are well fitted with the Gaussian distribution except the case of dry and naturally charged fibers smaller than 20 μm where the fitting is poor due to the high uniform background for the short fibers. Note that the Gaussian fits for humid and naturally charged fibers are good; R-square values are 0.9497, 0.9380, and 0.9731, and standard deviations are 13.7°, 12.9° and 15.6° for all lengths, L $<$ 20 μm, and L $>$ 20 μm, respectively.

Figure S5 shows that neutralizing the fibers to a Boltzmann charge distribution appears to broaden the alignment peak and also to enhance the uniform background of un-oriented fibers. The aligned peak of the long fibers (Figure S5c) is more pronounced relative to the uniform background compared to the short fibers (Figure S5b).

3.2.4. Effect of charging state on fiber alignment in humid condition

Figure S6 shows angular distribution of non-charged fibers in electric field in humid air. We assume that the electrostatic precipitator used to remove the charged fibers have a high removal efficiency close to 100%. It was found that the quality of the non-charged fiber alignment become lower than the charged as well as neutralized fibers, as shown in Figure S6. The background particles increased and the angular distribution became broader. Like the neutralized (Boltzmann) fibers in humid condition, the alignment of the non-charged short fibers tends to be much broader (i.e., standard deviation is 38.1°), indicating that it may not be easy for the neutralized and non-charged short fibers to be aligned completely. The angular distribution of the non-charged fibers with all lengths seems to be a little bit asymmetric around 90 degrees. Based on the fact that short fibers (Figure S6b) shows skewed angular distribution, but the long fibers show a symmetric Gaussian fit (Figure S6c), some instability might have happened to the short fibers. It is not clear what caused the asymmetry of the distribution. The quality of the fiber alignment in humid air, i.e., sharp peak and little background, is in the order of charged, neutralized, and non-charged fibers from best to worst. This result shows that the charge on the fibers affects the fiber alignment in humid condition.

4. Discussion

We directly demonstrated the electric field-driven alignment of aerosolized glass fibers. Specifically, we found out that under all four conditions tested above (i.e., dry and naturally charged, humid and naturally charged, humid and neutralized, and humid and non-charged), airborne glass fibers could align in the electric field, indicating that the glass fibers can behave in a steady electric field somewhat like conductors of electricity. In high humidity (RH = 90%), even short fibers could be aligned. Under dry conditions, alignment was less complete (broader peak with higher uniform background in the angular distribution, as shown in Table 1). In general, glass fibers are known to be poor electrical conductors, which are called a dielectric whose dielectric constant is about 5. It is worth noting that even though glass fibers are very nonconductive, i.e., dielectric particles, they can be aligned even in dry and naturally charged condition. This indicates that the glass fibers were polarized by the electric field in a steady state electric, and the torque exerted by electric field, rotating the fibers to the field, is big enough to overcome randomizing instabilities such as rotational Brownian motion in the space of electric field. However, it is worth noting that there is non-negligible background in the fiber angular distribution under dry and naturally charged condition as shown in Table 1, indicating that some fibers are randomly oriented in the field because they do not have strong polarization and rotating torque in the condition. Our data shows that this random orientation is more prominent for shorter

fibers than longer fibers; the fraction of background particles (i.e., randomly oriented fibers) for short fibers (L < 20 μm) in dry condition is 0.044, which is 42% higher than the one of 0.031 for long fibers (L > 20 μm), as shown in Table 1. This phenomenon is consistent with the study of Lilienfeld (1985) reporting that as fiber length decreases the electric field needed for keeping alignment increases for a given fiber length-to-diameter ratio. In addition, our data for dry and naturally charged fibers is supported by the study of Kwaadgras et al. (2011); Kwaadgras et al. (2011) numerically analyzed polarizability and alignment of dielectric rod-shaped nanoparticles in an external electric field to determine cluster dimension for which the energy difference associated with turning a nanocluster from its least to its most favorable orientation in a homogeneous static electric field exceeds the thermal energy such that particle alignment by the field is possible. They concluded that for the dielectric nanorod (silica) with an aspect ratio of 10, the longest dimension for which it might be aligned in the electric field (1 kV/cm) is about 1 μm. In other words, dielectric nanorods may not easily aligned by the external electric field because of their small size and low polarizability. In line with this fact, the short fibers (L < 20 μm) under dry and naturally charged condition in our study show a higher fraction of background particles in the angular distribution than the long fibers, indicating a low probability of their alignment in the electric field due to the random bombardment of gas molecules (i.e., Brownian motion) surrounding the fibers (Lilienfeld 1985).

It was found that there exist about one-third of the total number of the naturally charged fibers analyzed which are randomly oriented in the electric field in dry air. There are several factors which make fibers randomly orient; rotational Brownian motion, lack of polarized charges on the fiber ends, viscous drag of the air near the walls of electrodes and/or local micro-flow instability. It was suspected that a developing flow field (i.e., entrance effect) in the test unit (Figure 1) where the flow expanded and the parallel electrodes were installed, even though it is laminar, might interfere fiber alignment. So we tested this entrance effect of the flow with long entry length prior to the inlet of the test unit. We found that the entrance effect was somewhat reduced with the long entrance length before the unit, resulting in better alignment of fibers.

It is suspected that inhomogeneous charge distribution on the surface of the fibers may have happened probably because the charges attained by the glass fibers through the vortex shaking, i.e., triboelectric charging, could be immobile due to their non-conducting property; thus, this may cause fibers to have net charge on one end of the fibers relative to the other end of the fibers. We postulate that this non-uniform charge distribution of the glass fibers, unlike conductive fibers, might have exerted the rotating torque to the fiber resulting in fiber alignment in dry air.

The quality of fiber alignment in humid condition was found to be better than that in dry condition, as the humid and naturally charged fibers have the smallest standard deviation of the angular distribution, 12.9–15.6°, shown in Table 1. In humid condition, several mechanisms for enhanced polarization of the dielectric fibers have been suspected. The reason for the alignment of non-conducting fibers such as glass and asbestos in humid air has been postulated probably because of ionizing contaminants on the surface of the fibers (Fuchs 1964) or of water vapor adsorption (Lilienfeld 1985; Baron and Deye 1990). Wang et al. (2005) showed that humidity in air can change the electrical conductivity of glass fibers with indirect measurement in the Baron fiber classifier and argued that dissolving out soluble components from the glass surface might be the dominant process for conductance change. Pascal-Levy et al. (2012) performed measurements of charge distribution in between two grounded electrodes on an insulating layer surface of SiO_2 as a function of time when applying voltage to the SiO_2 surface at time = 0 s and showed that water molecules which adhere to the surface in ambient humidity conditions facilitate the movement of mobile charges on the SiO_2. The glass fibers used in our study consist of SiO_2 (61%), CaO (10.0%), Na_2O (15%), B_2O_3 (5.3%), Al_2O_3 (2.7%), MgO (2.5%) and other minor chemical components, according to analysis by Kohyama et al. (1997). It is known that all oxides are insoluble except those of calcium, barium and Alkali metal (Group I, i.e., Na^+) cations (AUS-e-TUTE 2014). Based on this fact about the solubility of oxides in water, we believe that soluble components such as CaO and Na_2O from the glass fiber surface might have dissolved in the water layer adsorbed on the surface, which would change the surface conductivity and make the fiber conducting. Chemical reaction between CaO and water vapor (H_2O) would happen: $CaO\ (s) + H_2O\ (l) = Ca(OH)_2\ (s)$, ($\Delta H = -64.8$ kJ/mol) and $Ca(OH)_2(s) \rightleftharpoons Ca^{2+}(aq) + 2\,OH^-(aq)$. The conductivity of the water film on the surface would depend on the ions (i.e., free ions such as OH^-) that may be released from the glass fiber when it is wetted. This explains why the glass fibers are aligned better to the electric field in humid air than in dry air. This observation in our study is in agreement with previous studies, which reported that humidity affects charge trapping by water molecules on SiO_2 surfaces exposed to the humid environment (Zhuravlev 2000; Pascal-Levy et al. 2012; Kim et al. 2003).

In order to support the above qualitative statements, we used the alignment energy equation and orientation probability as a result of polarizability to obtain a predicted orientation probability and compare it with measured orientation probability for humid data, assuming that fibers are conductive in the humid condition (so dielectric constant is infinite). The predicted orientation probability f(θ) that the angle between the fiber axis and the electric field direction lies in the interval (θ, θ+dθ) as a result of polarizability is expressed by Boltzmann's law (Fuchs 1964),

$$f(\theta) = \frac{e^{-\frac{U_p}{kT}}}{\int_0^{\pi} e^{-\frac{U_p}{kT}} \sin\theta \, d\theta} \quad [4]$$

where $\int_0^{\pi} f(\theta)\sin\theta \, d\theta = 1$, k Boltzmann constant, T absolute temperature, $U_p = -\frac{1}{2}E^2\cos^2\theta\left(\alpha_{\parallel} - \alpha_{\perp}\right)$, polarization energy for an axially symmetric particle with polarizability α (Bottcher and Belle 1973) and $\alpha_{\perp}$ and $\alpha_{||}$ are the principal component of polarization perpendicular to the axial direction and the component parallel to the axial direction, respectively.

Following the approximation used by Li et al. (2012) for the polarization energy of a fiber with that of a prolate spheroid and using λ (see below the definition of λ) for conducting fiber, the orientation probability becomes

$$f(\theta) = \frac{e^{\lambda^2\cos^2\theta}}{\int_0^{\pi} e^{\lambda^2\cos^2\theta}\sin\theta \, d\theta} \quad [5]$$

Finally, f(θ) is given by the following.

$$f(\theta) = \frac{e^{\lambda^2\cos^2\theta}}{\frac{\sqrt{\pi}}{\lambda} Erfi(\lambda)} \quad [6]$$

where $Erfi(t) = \frac{2}{\sqrt{\pi}}\int_0^t e^{x^2} dx$, the imaginary error function, and λ is a parameter which depends on electric field and polarizability, which is defined as

$$\lambda^2 = \frac{E^2}{2kT}\varepsilon_0 v\left(\frac{1}{\zeta_1} - \frac{1}{\zeta_2}\right) \quad [7]$$

where E is the electric field, v fiber volume, ε_0 permittivity of free space, and ζ shape factors.

Figure 8a and b show normalized measured and predicted orientation probability for humid data.

As λ increases, i.e., E or v increases, the orientation probability distribution becomes narrow. In other word, higher electric field and longer fibers tend to increase the orientation probability. The naturally charged fibers have a narrower orientation probability than the non-charged fibers, as the predicted orientation probability indicates in Figure 8. The corresponding values of lambda (λ) for 10 μm conducting charged and non-charged fibers are about 5.0 and 2.5, respectively for ~ 1000 V/cm. Figure 8 shows that the predicted orientation probability over-estimates the orientation effect; i.e. there are more fibers un-oriented at the larger angles ('in the wings') than are predicted by (6). It also should be noted that the orientation profiles (Figures 6b and d, 7a–c, and 8a and b) all exhibit sharp cusp-like behavior in the alignment direction, another feature not predicted by (6).

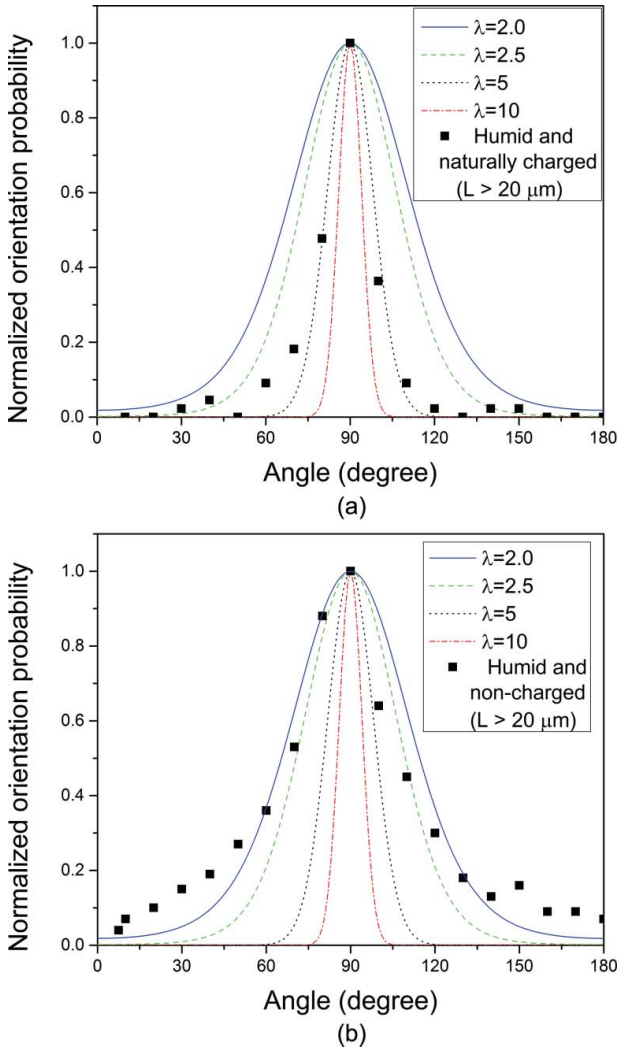

Figure 8. Normalized predicted and measured orientation probability in humid condition. (a) Naturally charged fibers > 20 μm and (b) non-charged fibers > 20 μm. Solid lines are for predicted values and square symbol is for measured one.

Now we are going to look at the charge effect on the fiber alignment. It was found that the charge state can also affect fiber alignment in our study; charged fibers in humid air can be more strongly aligned than neutralized

and non-charged fibers. The measured standard deviations of the angular distributions are 13.7°, 39.6° and 34.7°, and the R-square values are 0.9497, 0.8285, and 0.8490 for the charged, neutralized, and non-charged fibers, respectively (Table 1). The charge on the surface of the fibers might be molecular ions or small clusters generated by friction when being agitated by vortex shaking. This enhanced alignment by the fiber charge may be explained using the concept of heterogeneous nucleation of charged ions and non-charged molecules or nanoparticles. Winkler et al. (2008) showed that the charged particles are more easily activated for growth than neutral particles at diameter below 3 nm, and that the presence of ions, and electric charge on particles, would enhance the growth rates of very small nanoparticles and air ions. In our study the charged fibers in high humidity (90%) may have experienced a similar effect on the locations of charge; the condensing vapor (i.e., water vapor) may exhibit dipole nature and can thus be electrostatistically attracted to the charged fibers. The more charge on the surface of the fiber, the faster the fiber is coated by water vapor, making the fibers conducting enough to be aligned to the electric field.

Based on the fact that the glass fibers can align in the electric field, as shown with direct observation of fiber alignment in our study, although they are very poor conductors of electricity, it is expected that a similar phenomenon probably may occur in fibrous particles of other non-conducting materials with surface chemistry similar to glass fibers, especially in humid air condition. It is clear that the degree to which fibers can be aligned to an applied electric field will depend on surface properties of fibers, e.g., surface charge and surface conductivity due to water layer formation on the surface. Further study would be valuable to investigate the effect of surface properties of other fibers in dry and humid conditions on fiber alignment.

5. Conclusions

We directly demonstrated the electric field-driven alignment of aerosolized glass fibers by visualizing the fibers using phase contrast microscopy and measuring the angular distributions of the fibers. Specifically, we found out that under all four conditions tested (i.e., dry and naturally charged, humid and naturally charged, humid and neutralized, and humid and non-charged), airborne glass fibers could align in the electric field with different alignment quality even though they are non-conducting fibers. In humid air, the fiber alignment along the field direction is sharper and the uniform background in the angular distribution is smaller than in dry air. Also, it was found that charged fibers in humid air could be better aligned with negligible uniform background than neutralized and non-charged fibers. Possible mechanisms about humidity and charge effects on enhanced fiber alignment were discussed to explain the observations. The measured orientation probability (i.e., angular distribution) of the charged or non-charged fibers in humid air was compared with a predicted alignment probability to support the qualitative discussion. The results indicate that the enhancement of alignment in an electric field would be possible in humid air for other non-conducting fibrous particles having surface chemistry similar to glass fibers.

Acknowledgments

The authors thank Mariko Ono-Ogasawara (Japan National Institute of Occupational Safety and Health) for the samples of the GW1 glass fibers used in this study from Japan Fibrous Material Research Association (JFMRA). We thank Cara S. Lauber (Texas Tech University), for assisting in the analysis of PCM images of the fibers. We thank Chaolong Qi, Art Miller and Eileen Birch for helpful comments on this manuscript. We thank the referee of our manuscript for providing the alignment energy equation and orientation probability, supporting the qualitative discussion.

Funding

This work was funded by the NORA program at NIOSH. The findings and conclusions in this report are those of the authors and do not necessarily represent the views of the National Institute for Occupational Safety and Health. Mention of product or company name does not constitute endorsement by the Centers for Disease Control and Prevention.

References

Asgharian, B. and Yu, C. P. (1989). A Simplified Model of Interceptional Deposition of Fibers at Airway Bifurcations. *Aerosol Sci Technol.*, 11:1, 80–88.

AUS-e-TUTE. http://www.ausetute.com.au/solrules.html. Accessed Oct 3, 2014.

Baron, P. A. and Deye, G. J. (1990). Electrostatic Effects in Asbestos Sampling. I: Experimental Measurements. *Am. Ind. Hyg. Assoc. J.*, 51:51–62.

Baron, P. A., Deye, G. J., and Fernback, J. (1994). Length Separation of Fibers, *Aerosol Sci. Technol.*, 21(2):179–192

Bernstein, O. and Shapiro, M. (1994). Direct Determination of the Orientation Distribution Function of Cylindrical Particles Immersed in Laminar and Turbulent Shear Flows. *J. Aerosol Sci.*, 25:113–136.

Blake, T., Castranova, V., Schwegler-Berry, D., Deye, G. J., Baron, P., Li, C., and Jones, W. (1997). Effect of Fiber Length on Glass Microfiber Cytotoxicity. *J. Tox Environ. Health* 54A:243–59.

Bottcher, C. J. F. and Belle, O. C. V. (1973). Dielectrics in Static Fields. Elsevier Scientific Publishing Co., Amsterdam, NY.

Bubke, K., Gnewuch, H., Hempstead, M., Hammer, J., and Green, M. L. H. (1997). Optical Anisotropy of Dispersed Carbon Nanotubes Induced by an Electric Field. *Appl. Phys. Lett.*, 71:1906–1908.

Deye, G. J., Gao, P., Baron, P. A., and Fernback, J. (1999). Performance Evaluation of a Fiber Length Classifier. *Aerosol Sci. Technol.*, 30:420–437.

Fuchs, N. A. (1964). The Mechanics of Aerosols. Pergamon Press, Oxford.

Kapustin, V. N. and Covert, D. S. (1980). Measurements of the Humidification Processes of Hydroscopic Particles. *Appl. Optics*, 19:1349–1352.

Kapustin, V. N., Rozenberg, G. V., Ahlquist, N. C., Covert, D. S., Waggoner, A. P., and Charlson, R. J. (1980). Characterization of Nonspherical Atmospheric Aerosol-Particles with Electrooptical Nephelometry. *Appl. Optics*, 19:1345–1348.

Kim, S. H., Mulholland, G. W., and Zachariah, M. R. (2007). Understanding Ion-Mobility and Transport Properties of Aerosol Nanowires. *J. Aerosol. Sci.*, 38:823–842.

Kim, W., Javey, A., Vermesh, O., Wang, O., Li, Y. M., and Dai, H. J. (2003). Hysteresis Caused by Water Molecules in Carbon Nanotube Field-Effect Transistors. *Nano Lett.*, 3:193–198.

Kohyama, N., Tanaka, I., Tomita, M., Kudo, M., and Shinohara, Y. (1997). Preparation and Characteristics of Standard Reference Samples of Fibrous Minerals for Biological Experiments. *Ind. Health*, 35:415–432.

Ku, B. K., Deye, G., and Turkevich, L. A. (2013a). Characterization of a Vortex Shaking Method for Aerosolizing Fibers. The AAAR 2013 Conference Abstract, Sep 30 – Oct 4, 2013, Portland, OR.

Ku, B. K., Deye, G., and Turkevich, L. A. (2013b). Characterization of a Vortex Shaking Method for Aerosolizing Fibers. *Aerosol Sci. Technol.*, 47(12):1293–1301.

Ku, B. K., Deye, G. J., and Turkevich, L. A. (2014). Efficacy of Screens in Removing Long Fibers From an Aerosol Stream – Sample Preparation Technique for Toxicology Studies. *Inhal. Toxicol.*, 26:70–83.

Kwaadgras, B. W., Verdult, M., Dijkstra, M., and van Roij, R. (2011). Polarizability and Alignment of Dielectric Nanoparticles in an External Electric Field: Bowls, Dumbbells, and Cuboids. *J. Chem. Phys.*, 135: 135(13):134105

Li, M., Mulholland, G. W., and Zachariah, M. R. (2012). The Effect of Orientation on the Mobility and Dynamic Shape Factor of Charged Axially Symmetric Particles in an Electric Field. *Aerosol Sci. and Technol.*, 46(9):1035–1044.

Lilienfeld, P. (1985). Rotational Electrodynamics of Airborne Fibers. *J. Aerosol Sci.*, 16:315–322.

Lilienfeld, P. (1986). Optical-Detection of Particle Contamination on Surfaces – A Review. *Aerosol Sci. Tech.*, 5:145–165.

Lilienfeld, P. (1987). Light-Scattering from Oscillating Fibers at Normal Incidence. *J. Aerosol Sci.*, 18:389–400.

Lilienfeld, P., Elterman, P. B., and Baron, P. (1979). Development of a Prototype Fibrous Aerosol Monitor. *Am. Ind. Hyg. Assoc. J.*, 40:270–282.

Martin, C. A., Sandler, J. K. W., Windle, A. H., Schwarz, M. K., Bauhofer, W., Schulte, K., and Shaffer, M. S. P. (2005). Electric Field-Induced Aligned Multi-Wall Carbon Nanotube Networks in Epoxy Composites. *Polymer*, 46:877–886.

Monti, M., Natali, M., Torre, L., and Kenny, J. M. (2012). The Alignment of Single Walled Carbon Nanotubes in an Epoxy Resin by Applying a DC Electric Field. *Carbon*, 50:2453–2464.

Murugesh, A. K., Uthayanan, A., and Lekakou, C. (2010). Electrophoresis and Orientation of Multiple Wall Carbon Nanotubes in Polymer Solution. *Appl. Phys. a-Mater.*, 100:135–144.

Pascal-Levy, Y., Shifman, E., Sivan, I., Kalifa, I., Pal-Chowdhury, M., Shtempluck, O., Razin, A., Kochetkov, V., and Yaish, Y. E. (2012). Water Assisted Gate Induced Temporal Surface Charge Distribution Probed by Electrostatic Force Microscopy. *J. Appl. Phys.*, 112:084329.

Padmore, T., Stark, C., Turkevich, L. A., and Champion, J. A. (2017). Quantitative Analysis of the Role of Fiber Length on Phagocytosis and Inflammatory Response by Alveolar Macrophages. *Biochim. Biophys. Acta*, 1861:58–67.

Roschenko, A., Finlay, W. H., and Minev, P. D. (2011). The Aerodynamic Behaviour of Inhalable Fibers in a Linear Shear Flow. *Aerosol Sci. Tech.*, 45:1260–1271.

Takahashi, T., Murayama, T., Higuchi, A., Awano, H., and Yonetake, K. (2006). Aligning Vapor-Grown Carbon Fibers in Polydimethylsiloxane Using dc Electric or Magnetic Field. *Carbon*, 44:1180–1188.

Timbrell, V. (1975). Alignment of Respirable Asbestos Fibres by Magnetic Fields. *Ann. Occup. Hyg.*, 18 (4):299–311.

Wang, Z. C., Hopke, P. K., Baron, P. A., Ahmadi, G., Cheng, Y. S., Deye, G., and Su, W. C. (2005). Fiber Classification and the Influence of Average Air Humidity. *Aerosol Sci. Tech.*, 39:1056–1063.

Winkler, P. M., Steiner, G., Vrtala, A., Vehkamaki, H., Noppel, M., Lehtinen, K. E. J., Reischl, G. P., Wagner, P. E., and Kulmala, M. (2008). Heterogeneous Nucleation Experiments Bridging the Scale from Molecular Ion Clusters to Nanoparticles. *Science*, 319:1374–1377.

Zeidler-Erdely, P. C., Calhoun, W. J., Ameredes, B. T., et al. (2006). In vitro Cytotoxicity of Manville Code 100 Glass Fibers: Effect of Fiber Length on Human Alveolar Macrophages. *Part Fibre Toxicol*, 3:1–7.

Zhuravlev, L. T. (2000). The Surface Chemistry of Amorphous silica. Zhuravlev model. *Colloid Surface A*, 173:1–38.